A transient circuit model for a phase change memory element

H.G.A. Huizing[*], D. Tio Castro[*], J.C.J. Paasschens[**] and M.H.R. Lankhorst[***]

[*]Philips Research Europe,
Prof. Holstlaan 4, 5656AA Eindhoven, The Netherlands, bert.huizing@philips.com
[**] Philips Semiconductors, The Netherlands
[***]Now with Philips Lighting, The Netherlands

ABSTRACT

Non-volatile memories based on phase change materials (PCMs), also called 'Ovonic Unified Memories' (OUM), are promising candidates as a scalable and fast programmable alternative to existing memory concepts. We present a transient lumped element model of a phase change memory cell (PCMC). It can be used in a circuit simulator to optimize an OUM. The model is physics-based and describes typical features such as threshold voltage (V_T) switching. Also, and unlike existing circuit models [1,2], this model simulates V_T and resistance drift as found for PCMCs. All model parameters have physical meaning.

Keywords: circuit model, compact model, phase change memory cell

1 INTRODUCTION

Soon after the first publications on phase-change materials in the late 1960's [3], it was recognized that non-volatile and electrically programmable memories could be made using such materials. Recently, PCM-materials have been integrated into IC-technologies [4,5,6]. Existing memory concepts fail to scale in the ongoing quest of downsizing the memory elements. With PCM-technology, a scalable memory concept is anticipated.

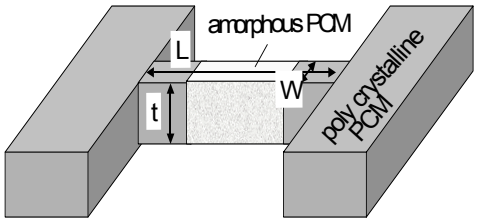

Figure 1. Line concept phase change cell.

A PCMC is in either a high-ohmic amorphous (RESET) state or in a low-ohmic crystalline (SET) state. Switching between the states is achieved by joule heating: high powers lead to melting and rapid quenching preserves the amorphous state. At moderate power levels the PCMC crystallizes. In figure 1, a schematic of a 'line-concept' cell is shown. Current is run through the line to heat it up and change its state.

A typical feature of PCM-materials that is employed during programming, is its 'threshold voltage switching' behavior. In the amorphous state, the I(V)-characteristics show 'snapback': beyond V_T the device breaks down and snaps back to join the same I(V)-curve as the crystalline state. V_T and R_{RESET} vary over time and depend on the switching history. V_T reduces just after a switching event and only slowly recovers [7] (see figure 2). This effect is particularly awkward in OUM-design as it puts constraints on the readout voltage and currents.

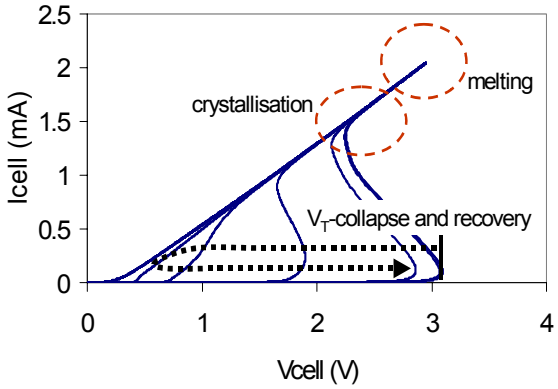

Figure 2. Qualitative illustration of the switching characteristics of an amorphous cell showing the typical snapback behavior and V_T-recovery.

Pirovani *et al*. have developed a physical model for the PCMC that explains most of its electrical features [7]. Key issue is the switching-dependent appearance and disappearance of traps, associated with structural 'valence alternation pairs' (VAPs), determining V_T, R_{RESET} and their drift. Pirovano's model is implemented in a numerical device simulator.

To enable and optimize the design of driver circuitry for an OUM, we developed a transient circuit model for a single cell. In the next section, we will first describe the model. In section 3 we show an example simulation and a comparison with experiments, followed by conclusions in section 4.

2 MODEL DESCRIPTION

The model consists of two parts. A thermal network (figure 3) calculates the temperature distribution in the cell caused by joule heating. An electrical network (figure 4) describes the momentous resistance. We assume a simple line geometry and a growth-limited PCM (doped GeSbTe [8]). In such materials two amorphous/crystalline (a/c-) interfaces move 'up and down' the line during programming cycles (reflecting melting or crystallization).

The model keeps track of the location of the amorphous-crystalline interface $x_{a/c}$. The speed of $x_{a/c}$ depends on the local temperature $T(x_{a/c})$ (ref. [8] and figure 5). $T(x_{a/c})$ is determined from the thermal network. $x_{a/c}$ at the end of the programming cycle determines the PCMC-resistance and state.

2.1 Thermal network

The thermal network determines the temperature distribution inside PCMC. We solve the heat equation by using electrical equivalencies and describing the –distributed– thermal network as an electrical network. The thermal network should be dense enough to resolve the temperature profiles in the structure correctly. At each node in the model, power is generated by relating it to the joule heating in the device. In this paper, we apply the relatively simple model given in figure 3 to model the line concept cell.

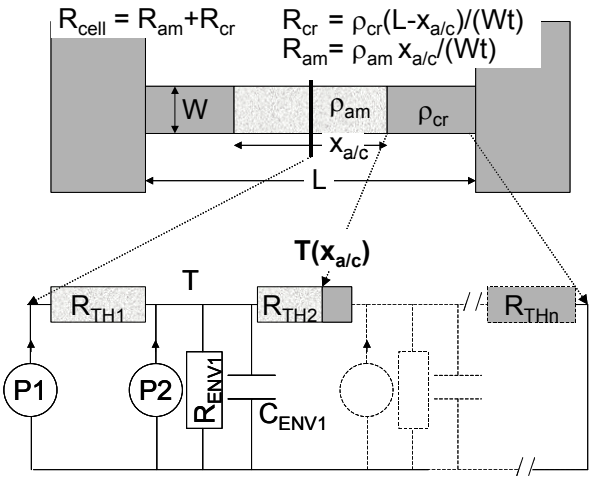

Figure 3. The model tracks the a/c-interface to calculate the cell resistance. A thermal network is implemented to calculate the temperature in the cell.

2.2 Electrical network

The electrical network (figure 4) consists of three resistances in series: the crystalline and amorphous part and a constant series resistance to account for any other resistance. The heat generated in the line is input to the thermal network, the heat in the series resistance not.

The crystalline resistance R_{cr} is modeled to be temperature dependent (in analogy with doped semiconductors).

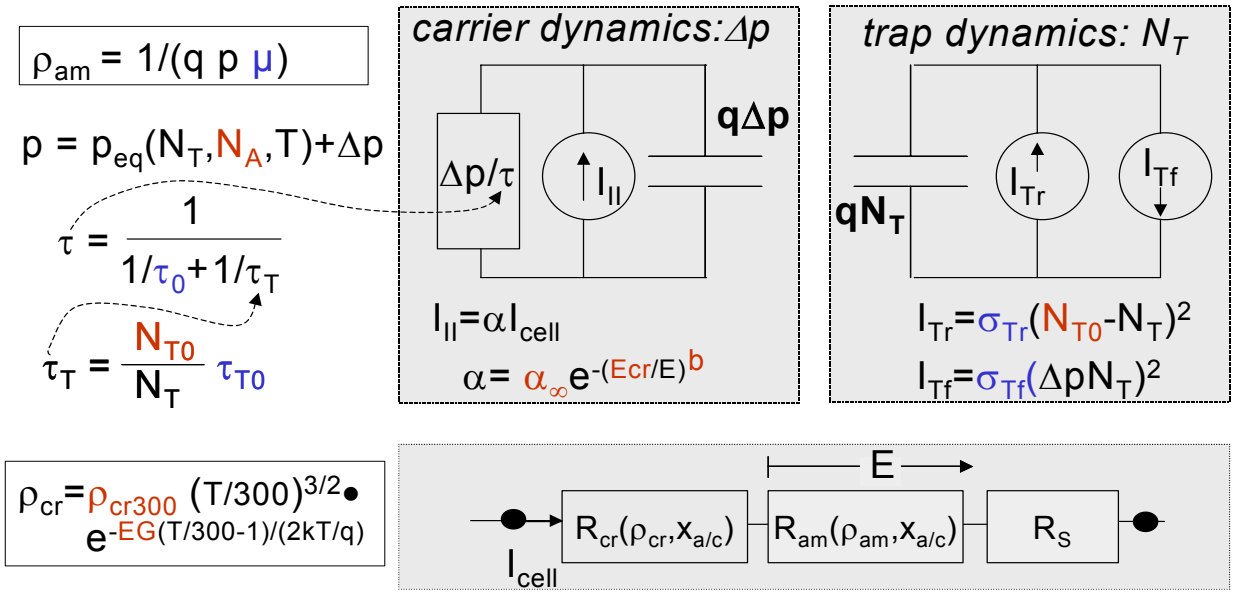

Figure 4. The electrical model consists of three resistances. Also, dummy networks are used to describe the carrier and trap dynamics. Resistivity ρ_{cr300}, bandgap E_G and breakdown parameters α_∞, E_{cr}, and b, as well as N_{T0} and doping N_A are considered material parameters that can be independently determined. Mobility μ and lifetimes and reaction rates τ_0, τ_{T0}, σ_{TF} and σ_{Tr} also have physical meaning, but are to date determined by calibration of the model to cell measurement data.

To model the more complicated behavior of the amorphous resistance R_{am}, impact ionization and recombination effects are included. In this paper, conduction is assumed to take place primarily by holes as it is believed that the hole mobility is larger then the electron mobility. This is, however, not essential to the model. To calculate R_{am}, the hole concentration p must be known, as we will calculate the specific resistance from $\rho_{am} = 1/(q\mu_p p)$, with q being the elemental charge and μ_p the hole mobility. We assume p is constant in the amorphous region. Next, we write $p=\Delta p+p_{eq}$, with p_{eq} being the –background– hole concentration of the material at zero and low currents and Δp the excess hole concentration due to breakdown. We keep track of Δp and p_{eq}.

The excess hole concentration Δp is calculated in a

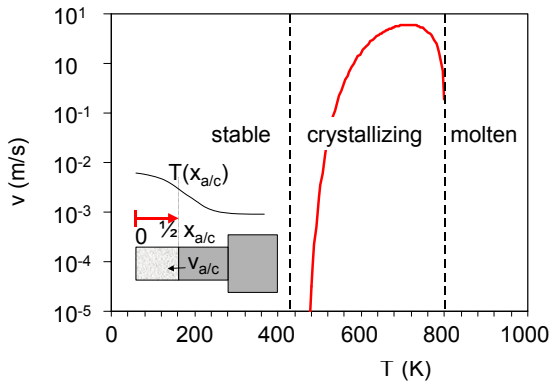

Figure 5. Model for crystallization speed of the a/c-interface in a growth limited phase change material (physical expression calibrated to measurements).

dummy network (figure 4) where a capacitor is charged by 'current sources' representing the competing mechanisms of impact ionization and recombination through traps. The rate of recombination is determined by the trap concentration N_T and associated lifetime τ_{T0}. A complication arises from the fact that the traps disappear quite suddenly when the device breaks down. The traps return only slowly to their equilibrium concentration N_{T0}, which is assumed to be equal to twice the concentration of VAPs. To model the dis- and reappearance of traps, the trap dynamics are included in the model. Similar to Δp, N_T is calculated using a dummy network where the charge on a capacitor is a measure for N_T. At breakdown, the VAPs reconfigure, forced by an abundance of holes and electrons, from a donor and acceptor trap C_3^+ and C_1^- into two non-trapping states C_3^0, see Adler [9] and Pirovano [7]. The implemented reaction is therefore:

$$h^+ + e^- + C_3^+ + C_1^- \leftrightarrow 2C_3^0 \tag{1}$$

If we further assume that C_3^+ and C_1^- cannot live separate lives (being a VAP), we may assume $[C_3^+] = [C_1^-] \equiv N_T$. Next realizing that $[C_3^0]=N_{T0}-N_T$ we arrive at:

$$\frac{dN_T}{dt} = \sigma_f pnN_T^2 - \sigma_r\left(N_{T0} - N_T\right)^2 \tag{2}$$

where σ_f and σ_r are the forward and reverse reaction rates. In breakdown, $p \approx n \approx \Delta p$ and we may rewrite this to:

$$\frac{dN_T}{dt} = \sigma_f\left(\Delta pN_T\right)^2 - \sigma_r\left(N_{T0} - N_T\right)^2 \tag{3}$$

The equilibrium hole concentration p_{eq}, as well as electron concentration n_{eq}, are calculated using Boltzmann statistics including the contribution of doping and traps. Using standard text-book formulae for solid state semiconductors we write:

$$\begin{aligned} n_{eq} &= N_C e^{E_F/U_T} \\ p_{eq} &= N_V e^{-(EG+E_F)/U_T} \\ N_A^- &= N_A \frac{1}{1+4e^{(E_A-E_F)/U_T}} \\ N_{TD}^+ &= N_T \frac{1}{1+2e^{(E_F-E_{TD})/U_T}} \\ N_{TA}^- &= N_T \frac{1}{1+4e^{(E_{TA}-E_F)/U_T}} \end{aligned} \tag{4}$$

where N_C and N_V are the effective density of states, U_T the thermal voltage kT/q, N_A the hole doping level and N_{TD}^+ and N_{TA}^- the charged trap concentrations. In this paper, the acceptor level E_A is chosen to be very close to the valence band so that in practice $N_A^- \approx N_A$. The trap energies E_{TD} and E_{TA} are set to the same midgap state. The Fermi level E_F is solved within the model by applying the 'charge neutral' condition:

$$n_{eq} + N_A^- + N_{TA}^- = p_{eq} + N_{TD}^+ \tag{5}$$

p_{eq} is thus known. Through N_{TA}^- and N_{TD}^+ it is obvious that the trap concentration plays a role in determining p_{eq}, and hence R_{RESET}. N_T also determines V_T through its effect on the carrier lifetime τ_T. Drift of both R_{RESET} and V_T is thus quite naturally modeled by keeping track of the momentous trap concentration. When the device breaks down, all traps disappear and the lifetime becomes high: V_T is low. Also, N_{TD}^+ and N_{TA}^- become low and the Fermi level moves to E_A and thus near the valence band. This

results in a higher p_{eq}, i.e. lower R_{RESET}. When the traps reappear over time, the lifetime will decrease again and V_T will recover. Also, E_F moves back towards the trap level, which means a lower p_{eq} and increasing R_{RESET}. A 'residual' lifetime τ_0 is included in the model, not related to valence alternation pairs, to avoid the lifetime becoming infinite. τ_0 sets the apparent holding voltage of the device.

3 SIMULATION RESULTS

Simulation results are given in figures 6 and 7. In figure 6, we show the drift of V_T and R_{RESET} after a breakdown event. A device with L×W=80×20nm^2 is measured and

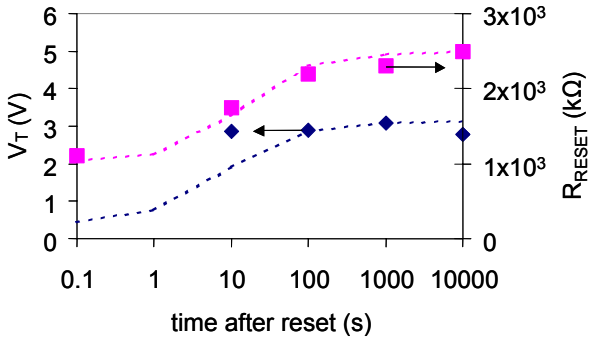

Figure 6. V_T and R_{RESET} drift, as caused by trap dynamics. Dashed line are simulations, the symbols are measurements for a 80x20nm^2 device

simulated. Measurements are done with 6V triangular, 100ns wide pulses with a series resistance of 1kΩ. The measured V_T's are taken from dynamic IV-curves with an

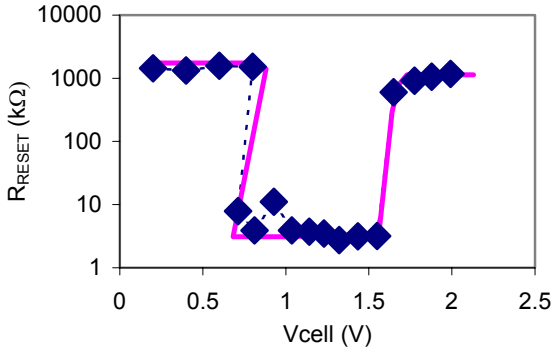

Figure 7. Programming curve for a device (80x20nm^2) in amorphous state. Symbols are measurements, the solid line is the simulation result. Vcell is the voltage across the phase change cell.

accuracy of +- 0.1-0.2 V. Figure 7 shows the programming curve for the same device. Each data point is measured in a sequence of three pulses: first a large pulse to completely amorphize the line, followed immediately by a square programming pulse of 100ns wide, followed finally by a small read pulse to determine R_{RESET}. As in figure 6, the programming is done with 1kΩ series resistance. The second pulse was increased to determine each data point. The actual voltage Vcell across the cell is measured. A transient simulation to determine one data point in figure 7 involved ~2500 time steps and took 5-15 seconds to calculate in a circuit simulator on a linux-based state-of-the-art pc.

The model is able to capture all features in the measurements.

4 CONCLUSION

In conclusion, we have developed a physics based transient circuit model for a phase change memory cell. It captures all relevant features, including threshold switching and drift of the threshold voltage and resistance. The model is fast and can be used in a circuit simulator.

REFERENCES

[1] X.Q. Wei et al., *Universal HSPICE model for chalcogenide based phase change memory elements,* Non-Volatile Memory Technology Symposium 2004, p.88.

[2] R.A. Cobly, C.D. Wright, *SPICE modeling of PCRAM devices*, Proc.-Sci. Meas. Techn. Vol. 150, 2003, p.237.

[3] S.R. Ovshinky, *Reversible Electrical Switching Phenomena in Disordered Structures*, Phys. Rev. Lett. 21, 1968, p. 1450.

[4] W.Y. Cho et al., *A 0.18 pm 3.0 V 64Mb non-volatile phase-transition random-access memory (PRAM)*, IEEE Solid-State Circuits Conference 2004, p. 40.

[5] S. Lai, *Current status of the phase change memory and its future*, Int. Electr. Dev. Meeting, 2003, p. 255.

[6] F. Bedeschi et al., *4-Mb MOSFET-selected phase-change memory experimental chip*, European Solid-State Circuits Conference, 2004, p. 207.

[7] A. Pirovano et al., *Low-Field amorphous state resistance and voltage drift in chalcogenide materials*, IEEE TED, Vol. 51, 2004, p. 714.

[8] M.H.R. Lankhorst et al. *Low-Cost and nano-scale nonvolatile memory concepts for future silicon chips*, Nature Materials 4, 2005, p. 4.

[9] D. Adler et al. *Threshold voltage switching in chalcogenide-glass thin films*, J. Appl. Phys, vol. 51, 1980, p. 3289.